Moment ratios and dynamic critical behavior of a reactive system with several absorbing configurations

M. F. de Andrade and W. Figueiredo
Departamento de Física, Universidade Federal de Santa Catarina, 88040-900, Florianópolis, SC, Brazil.
(Received 10 November 2010; revised manuscript received 28 January 2011; published 9 March 2011; publisher error corrected 15 March 2011)

We determine the critical behavior of a reactive model with many absorbing configurations. Monomers A and B land on the sites of a linear lattice and can react depending on the state of their nearest-neighbor sites. The probability of a reaction depends on temperature of the catalyst as well as on the energy coupling between pairs of nearest-neighbor monomers. We employ Monte Carlo simulations to calculate the moments of the order parameter of the model as a function of temperature. Some ratios between pairs of moments are independent of temperature and are in the same universality class of the contact process. We also find the dynamical critical exponents of the model and we show that they are in the directed percolation universality class whatever the values of temperature.

DOI: 10.1103/PhysRevE.83.031108 PACS number(s): 05.70.Ln, 05.70.Jk, 64.60.Ht, 68.35.Rh

I. INTRODUCTION

In a recent paper [1] we investigated the static properties of a reaction model between pairs of monomers A and B on a linear lattice, where we considered lateral interactions between nearest-neighbor adsorbed species as well as thermal effects. The phase diagram of the model was determined and we observed that, depending on temperature, the absorbing state is a poisoned state with different concentrations of monomers A and B. In spite of this fact, the static critical exponents of the model are in the same universality class of the directed percolation (DP) [2,3]. The DP is the fundamental universality class related to absorbing phase transitions. A set of static and dynamic critical exponents, which are in full agreement with those defining the DP in $(2+1)$ dimensions, were recently obtained in an experiment concerning different phases of a liquid crystal [4,5]. The task of devising experimental phase transitions to absorbing states is very complex, because in real systems the presence of impurities and other inhomogeneities [6] hinders large fluctuations.

Amongst the several models displaying transitions to absorbing states, the contact process (CP) is the simplest one that undergoes this kind of transition. This model was proposed to mimic the spreading of a disease [7], and its dynamics are driven by the rate of change of healthy individuals into unhealthy ones. Surface catalytic reaction models [8], transition to turbulence [9], and traffic flow [10] are also examples where one can find transitions to an absorbing state.

The model proposed by Ziff, Gulari, and Barshad [8] to explain the oxidation of the carbon monoxide over a surface is the simplest model that exhibits first-order and continuous phase transitions to absorbing states. In the literature there are many other interesting examples of catalytic reaction models with phase transitions from active to absorbing states [11–14]. In particular, we are interested in the study of catalytic reaction models with competitive reactions between two types of monomers: the autocatalytic reaction $A + A \rightarrow A_2$ [15] and the simple monomer-monomer reaction $A + B \rightarrow AB$ [16]. This competitive reaction model was studied, at zero temperature, through the dynamical mean-field approximation and Monte Carlo simulations [17,18]. The results showed that the critical exponents of the model are in the DP universality class, and that the absorbing state is unique, with the lattice completely poisoned by monomers of type B. The consideration of thermal effects into this model produces a multitude of absorbing configurations; however, the DP universality class is preserved regarding its static critical properties [1].

A question arises concerning the dynamical critical exponents of the model. As shown by Mendes *et al.* [19], transition into a nonunique absorbing state may exhibit nonuniversal behavior regarding the dynamical critical exponents. They generalized the scaling theory to take into account exponents that can change with the initial configuration. As the model we studied recently presents different absorbing configurations, we decided to investigate its dynamical critical exponents in order to see if they are dependent on the starting configuration. In order to accomplish this we revisit our model and calculate its corresponding dynamical critical exponents as a function of temperature, which is equivalent to changing the nature of the absorbing state. We also calculate the moment ratios between some moments of the order parameter to tune the critical point for each value of temperature. The critical point agrees with the values we have found in our previous work [1] and, for all considered temperatures, the dynamical critical exponents of the model are in the DP universality class. Special attention is also paid to the spreading dynamics, since the initial condition could affect the dynamical critical exponents δ, η, and ζ, as pointed out by Mendes *et al.* [19].

This paper is organized as follows: in the next section we define the model and its energy parameters. In Sec. III we present the details related to the moment ratios calculations. In Sec. IV, we start our time-dependent calculations, determining the dynamic exponent z. In Sec. V, we complete the discussion concerning the dynamic aspects of the model, performing a spreading analysis to calculate its dynamical exponents. Finally, in the last section, we present our main conclusions.

II. THE MODEL

In this study we consider a reaction model where two competitive reactions, the autocatalytic reaction $A + A \rightarrow A_2$

[15] and the monomer-monomer reaction $A + B \rightarrow AB$ [16], occur on a catalyst which is represented by a linear lattice. The monomers A and B arrive at the lattice, which is in contact with an infinite reservoir of monomers, with probabilities y_A and y_B respectively, where $y_A + y_B = 1$. These probabilities are related to the partial pressure of the gases inside the reservoir. Each monomer can occupy only a single vacant site in the lattice. The individual processes that can occur in our model are the following:

$$A_{(g)} + v \rightarrow A_{(a)}, \tag{1a}$$

$$B_{(g)} + v \rightarrow B_{(a)}, \tag{1b}$$

$$A_{(a)} + A_{(a)} \rightarrow A_{2_{(g)}} \uparrow, \tag{1c}$$

$$A_{(a)} + B_{(a)} \rightarrow AB_{(g)} \uparrow, \tag{1d}$$

where v represents a vacant site in the lattice and the labels (g) and (a) denote a monomer in the gaseous and adsorbed phases, respectively. The first two steps describe the adsorption of the species on the substrate, and the next two steps describe the possible reactions between adsorbed monomers occupying nearest-neighboring sites. Immediately after a reaction, A_2 or AB molecules go away from the catalyst and a pair of nearest-neighbor vacant sites is left on the substrate. Diffusion and desorption of the species are not take into account in this model.

Costa and Figueiredo [17] studied this model in the adsorption-controlled limit, where the reaction rates are much larger than the adsorption rates. In their model, monomer A always lands on the lattice and reacts quickly with one of its nearest neighbors if they are occupied by A or B monomers. The probability to react with an A monomer is the same as to react with a B monomer. This model exhibits a unique absorbing state, which is characterized by a lattice completely poisoned by monomers of type B. The steps $(1a)$–$(1d)$ are equivalent to a lattice model for the birth and death of vacancies, akin to the contact process. The processes $(1a)$ and $(1b)$ account for the annihilation of a vacancy due to the adsorption of a particle, while the processes $(1c)$ and $(1d)$ give the birth of a vacancy due to the reaction step. In this way, we can summarize the four steps above by a simple birth-death process for vacancies: $v \rightarrow \emptyset$ and $v \rightarrow 2v$.

As in our previous study concerning the static properties of the model, the temperature of the catalyst and interactions between nearest-neighbor adsorbed species are the main ingredients of the model. As a matter of fact, the adsorption process cannot occur, even if the chosen lattice site for deposition is empty. Every time we try to deposit a new monomer on an empty site of the lattice, we calculate the change ΔE in energy that this event would cause in the whole system. We assume that there is a repulsive energy ϵ ($\epsilon > 0$) between nearest-neighbor pairs of A monomers or A and B monomers, as well as between monomers and the catalyst. For any temperature, the probability that a B monomer is adsorbed is one, provided that its nearest neighbors are vacant sites or occupied by B monomers. On the other hand, an A monomer is always adsorbed if its nearest-neighbor sites are both empty.

The adsorption of a monomer occurs with probability

$$\frac{\exp[-E_a/(k_B T)]}{\exp[-E_a/(k_B T)] + \exp[-E_b/(k_B T)]}, \tag{2}$$

$$\left.\begin{array}{l} Avv \rightarrow AAv \\ Avv \rightarrow ABv \\ AvB \rightarrow ABB \end{array}\right\} \alpha = \frac{2}{1 + e^{2\varepsilon/k_B T}}$$

$$\left.\begin{array}{l} AvA \rightarrow AAA \\ AvB \rightarrow AAB \\ AvA \rightarrow ABA \\ BvB \rightarrow BAB \end{array}\right\} \alpha = \frac{2}{1 + e^{3\varepsilon/k_B T}}$$

FIG. 1. Transitions and their respective weights.

where E_a and E_b mean the energies after and before adsorption, respectively. Writing $\Delta E = (E_a - E_b)$, and introducing a factor 2 in the last equation to render probabilities in the range 0 to 1, we finally get the Boltzmann-like weight factor for the probability of an adsorption event:

$$\alpha = \frac{2}{1 + e^{+\Delta E/(k_B T)}}, \tag{3}$$

where the temperature T of the substrate is measured in units of ε/k_B, and k_B is the Boltzmann constant. In Fig. 1 we display a diagram illustrating the transitions for which the factor given by Eq. (3) is evaluated.

Then, due to the interaction-energy parameters of our model, we always have $\Delta E > 0$, which gives $\alpha \rightarrow 0$ when $T \rightarrow 0$ and $\alpha \rightarrow 1$ at high temperatures. If the monomer is not adsorbed, it reacts with probability $(1 - \alpha)$. This choice recovers, in the limit $T \rightarrow 0$, the model considered by Costa and Figueiredo [17] where the absorbing state is unique, corresponding to a lattice completely filled with B monomers. In that model, it is not possible for a monomer of type A to stay adsorbed in the presence of another A or B monomer, and Eq. (1), for $T \rightarrow 0$, is consistent with an absorbing state where the lattice is filled only with monomers of type B. Through mean-field calculations and Monte Carlo simulations we have seen that, at finite temperatures, the absorbing states depend on temperature. When temperature changes from zero to infinite we find that the absorbing state also changes continually from a pure B state to a pure A state. For finite values of temperature, the absorbing state is a mixture of A and B monomers, with fixed values of their concentrations, but with many different microscopic configurations of the species.

III. MOMENT RATIOS CALCULATIONS

From our previous results [1] concerning the critical values of the control parameter y_A we calculate the ratios between some moments of the order parameter n_v, which is the fraction of empty sites in the lattice. This approach was applied in the context of equilibrium systems [20] and, later, successfully extended to models out of equilibrium that present transitions to absorbing states [21–23]. The procedure is based on the fact that some ratios between different moments of the order parameter do not depend upon the system size at the critical point, showing universal values. The curves corresponding to these moment ratios for different system sizes cross themselves at the critical point where the transition from the active to the

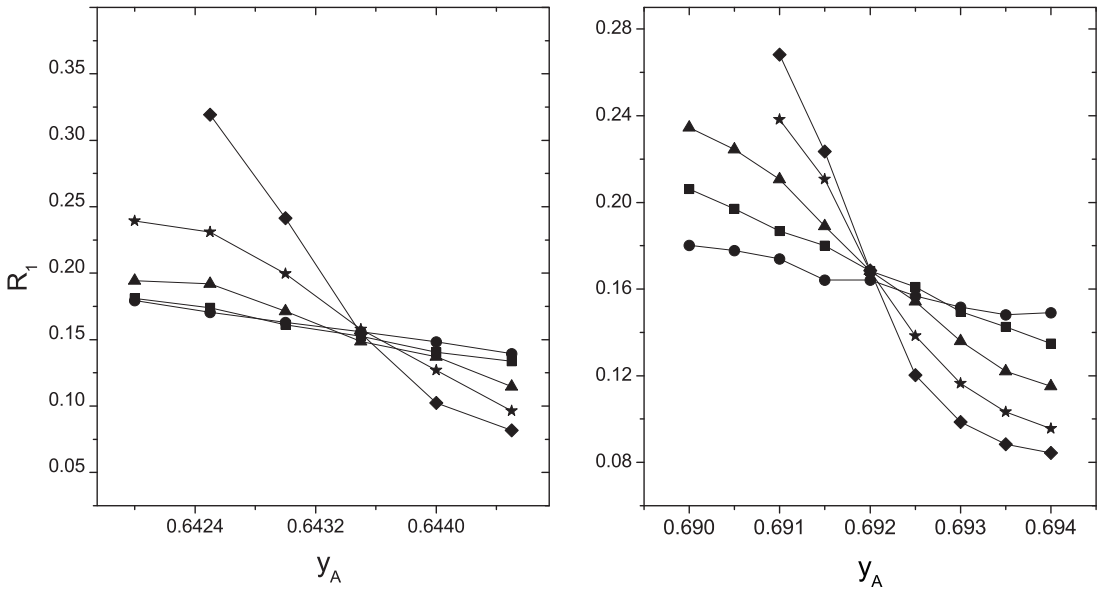

FIG. 2. Ratio R_1 versus y_A. Left panel shows results for $T = 0.5$ and the right panel for $T = 0.9$. The symbols are associated with different system sizes L as follows: ●= 256, ■= 512, ▲= 1024, ★ = 2048, ◆= 4096.

absorbing state occurs. The moments of the order parameter are defined by

$$m_k = \langle n_v^k \rangle, \tag{4}$$

where k indicates the order of the moment. We consider moments up to fourth order and the second-order cumulant $Q_2 = m_2 - m_1^2$. Static Monte Carlo simulations are then used to achieve the stationary states for different values of y_A and for system sizes ranging from $L = 256$ to $L = 4096$. It is worth mentioning that the only true stationary state is the absorbing one, since we are dealing with finite lattices. Actually, one must refer to the transition between absorbing and quasistationary states. We look for a time window where the system can be found in a stationary active state, and then calculate averages over several samples, taking into account only the surviving ones. The time spent by the system in the active phase depends on the system size L and on the distance from the critical point ($\Delta = y_A - y_{A_c}$). For large L and small Δ, the quasistationary order parameter can be written as

$$m_1(\Delta, L) \propto L^{-\beta/\nu_\perp} f(\Delta L^{1/\nu_\perp}), \tag{5}$$

where the scaling function $f(x) \propto x^\beta$ for large x, and β and $\nu_\perp$ are the critical exponents associated with the order parameter and the spatial correlation length, respectively. For $\Delta = 0$ we can write

$$m_1(0, L) \propto L^{-\beta/\nu_\perp}, \tag{6}$$

since $f(x) \approx 1$ when x approaches 0. To calculate higher-order moments it is useful to consider the probability distribution $P(n_v, L)$ for the density of empty sites at the critical point. The kth moment of the order parameter comes from

$$m_k = \int_0^1 n_v^k P(n_v, L) dn_v = I_k L^{-k\beta/\nu_\perp}, \tag{7}$$

where the quantity I_k does not depend upon L in the large-L limit. Thus, it is possible to write ratios between powers of some moments of the order parameter; for example,

$$\frac{m_k^r}{m_l^s} \propto L^{-(\beta/\nu_\perp)(kr - ls)}. \tag{8}$$

If we choose $kr = ls$, the ratio becomes independent of the system size at the critical point. In this scenario, plots of these ratios as function of the control parameter y_A will intercept themselves at the critical point for any L. We evaluated the following ratios for each temperature: $R_1 = Q_2/m_1^2$, $R_2 = m_4/m_2^2$, $R_3 = m_3/m_1^3$, $R_4 = m_3/m_1 m_1^2$, $R_5 = m_2/m_1^2$.

The simulations were carried out considering periodic boundary conditions and a lattice completely empty as the initial condition. In order to save computational time we applied a continuous-time algorithm. Instead of looking for an empty site in the whole lattice, we restrict our search to the sites of a list of empty sites at each instant of time. It is worthwhile because, close to absorbing states, the number of empty sites is very small. Thus, our Monte Carlo step (MCs) is a dynamic time unit. For the lattice size $L = 256$ and $T = 0.5$ we computed averages for 1.0×10^5 samples in the interval between 600 to 800 MCs, where the samples showed a quasistationary behavior. For $L = 4096$ and $T = 1.3$, we needed 1.0×10^3 samples in the interval 9.0×10^3 to 1.2×10^4 MCs. From these averages we determined the mean fraction of empty sites for each y_A, T, and L. Figure 2 shows the ratio R_1 versus y_A for different system sizes and temperatures $T = 0.5$ and $T = 0.9$.

For the temperature $T = 0.5$ and for all lattice sizes, they cross themselves at $y_A = 0.6435$, and for $T = 0.9$ they cross at $y_A = 0.692$. In Fig. 3 we collect all these ratios for $T = 0.5$ at the critical point. There is a small dependence of the moment ratios on the lattice size L. By linearly extrapolating these ratios for $L \to \infty$ and considering only the three largest lattice sizes (i.e., $L = 1024$, 2048, and 4096), we determined the five

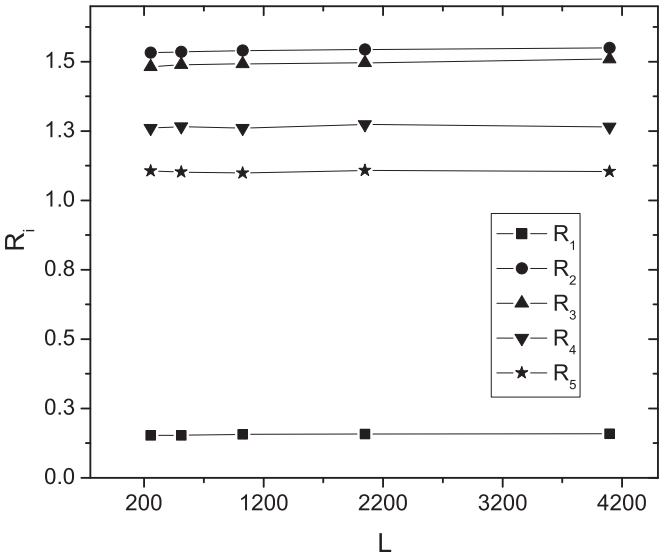

FIG. 3. Moment ratios as a function of the lattice size L at the critical point for $T = 0.5$.

ratios for four different temperatures. In Table I we summarize these results.

As we can see, these ratios do not depend on temperature and present universal values at the critical point. Within the uncertainty errors, the values we found are in close agreement with those determined for the contact process [21].

IV. DYNAMIC CRITICAL EXPONENTS

The mean time for a selected sample s to become poisoned is defined as

$$\tau_s = \frac{\sum_t t p_v}{\sum_t p_v}. \tag{9}$$

For each temperature the characteristic time τ_s is a function of the system size L and of the control parameter y_A. Averaging over all the samples we have $\tau = \langle \tau_s \rangle$, which is expected to follow the scaling relation [15]

$$\tau \sim L^z f\left(\Delta L^{1/\nu_\perp}\right), \tag{10}$$

where the scaling function f behaves as $f(0) \sim 1$. Thus, at the critical point, a log-log plot of τ versus the system size L is a straight line whose slope is the dynamical exponent z. We started the simulations with an empty lattice and recorded

TABLE I. Estimates of the moment ratios at the critical point for each temperature. We consider a range of temperatures from $T = 0.5$ up to $T = 1.3$, covering different regions of the phase diagram.

T	R_1	R_2	R_3	R_4	R_5
0.5	0.167(3)	1.551(2)	1.551(7)	1.291(6)	1.168(3)
0.9	0.166(4)	1.546(3)	1.515(4)	1.289(7)	1.169(2)
1.3	0.168(2)	1.548(3)	1.517(2)	1.296(4)	1.165(2)
1.33	0.169(3)	1.549(4)	1.511(6)	1.294(4)	1.169(3)
CP[21]	0.1736(2)	1.554(2)	1.523(6)	1.301(3)	-

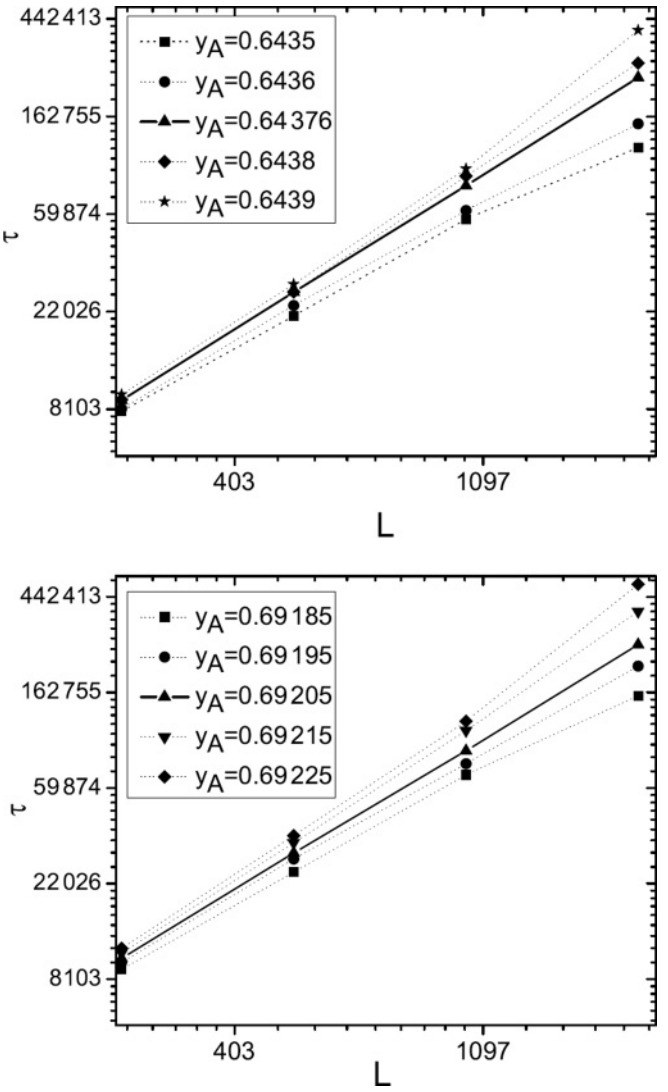

FIG. 4. Characteristic time τ versus system size L. The top figure displays the results for $T = 0.5$ and the bottom one for $T = 0.9$. The straight lines indicate the critical point and their slopes give the dynamical exponent z.

the time until the lattice becomes completely occupied by monomers A and B. By employing the critical values we found from the moment-ratio calculations, we simulated several samples close to the critical point. In this way we determined a more precise value for y_{A_c} and calculated the dynamical exponent z from the slope of the curve.

We show in Fig. 4 plots of τ against L for two temperatures. When $T = 0.5$ we have a straight line for $y_A = 0.643\,76$ and its slope is $z = 1.590(7)$, while for $T = 0.9$, $y_A = 0.692\,05$ and $z = 1.575(6)$. We also performed the calculation for other values of temperature. For instance, for $T = 1.3$, we have $y_A = 0.8693$ and $z = 1.583(8)$ and for $T = 1.33$, we have $y_A = 0.9262$ and $z = 1.584(7)$. We also observe that the dynamic exponent z does not depend on temperature and its values are, within the uncertainty errors, in good agreement with those of the DP universality class. In the next section we also investigate the dynamical critical behavior by means of an epidemic analysis.

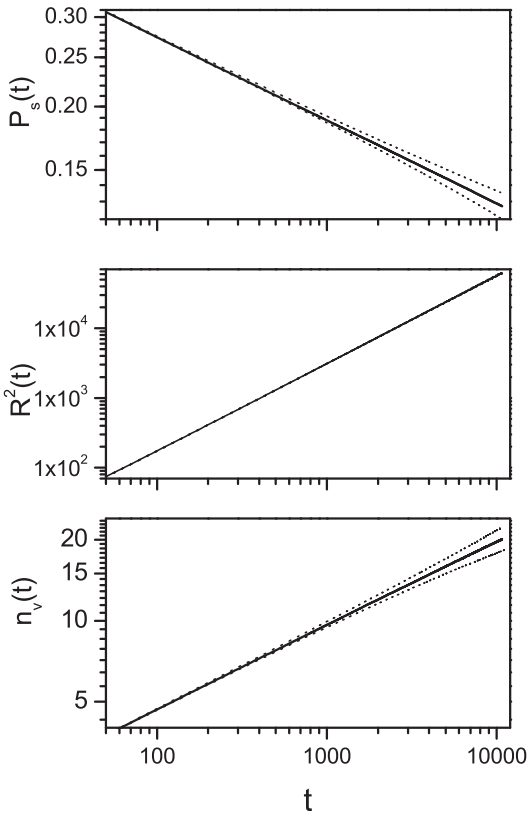

FIG. 5. $P_s(t)$, $R^2(t)$, and $n_v(t)$ versus t in log-log scale for $T = 0.5$. The curves are associated, from bottom to top, with the values $y_A = 0.6435$, $y_A = 0.6436$, and $y_A = 0.6437$. The central line defines the critical point.

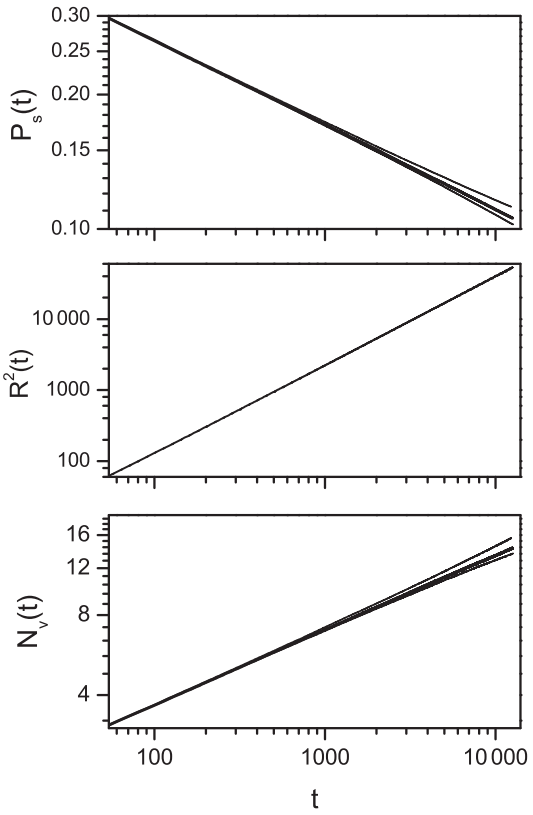

FIG. 6. $P_s(t)$, $R^2(t)$, and $n_v(t)$ versus t in log-log scale for $T = 0.9$. The curves are associated, from bottom to top, to the values $y_A = 0.69$, $y_A = 0.692\,05$, and $y_A = 0.693$

V. SPREADING DYNAMICS

Originally proposed by Grassberger and de la Torre [24], this method considers the evolution of the activity generated by a single seed in the lattice, very close to the absorbing state. In our case a single seed means one empty site at the center of a completely covered lattice. The quantities of interest are the survival probability $P_s(t)$, the mean number of empty sites $n_v(t)$, and the mean square displacement $R^2(t)$. Starting from an initial condition with only one empty site at the center of the lattice, we followed the time evolution of 2.6×10^6 independent samples until a maximum time $t = 1 \times 10^4$ MCs. We defined our time step as being 100 attempts to change the configuration of the lattice. In order to prevent boundary effects we simulate our system in a lattice of size $L = 5 \times 10^5$, so there will be no activity at the edges of the lattice for the time scale we are dealing with. It is worth mentioning that $n_v(t)$ is averaged over all the samples, while $P_s(t)$ and $R^2(t)$ are calculated only with those samples which have not reached the absorbing state at time t. Following Grassberger and de la Torre, we assume that the quantities of interest depend on the parameters t, $\Delta(\Delta = y_{A_c} - y_A)$, and $\vec{x}$, according to the scaling variables x^2/t^ζ and $\Delta t^{1/\nu_\parallel}$ times some power of t, Δ, or x^2. In the scaling regime, for large system sizes and long times, the conditional probability of finding an empty site at the position $\vec{x}$, provided that at $t = 0$ we had only one empty site at $\vec{x} = 0$, is given by

$$\rho\left(\vec{x},t\right) \approx t^{\eta - d\zeta/2} F(x^2/t^\zeta, \Delta t^{1/\nu_\parallel}), \tag{11}$$

where d is the system dimensionality. The survival probability can be written as

$$P_s(t) \approx t^{-\delta} \varphi\left(\Delta t^{\nu_\parallel}\right), \tag{12}$$

with $\nu_\parallel$ being the critical exponent associated to the temporal correlation length. From Eq. (11) we can write expressions for the mean number of empty sites:

$$n_v(t) = \int t^{\eta - d\zeta/2} F(x^2/t^\zeta, \Delta t^{1/\nu_\parallel}) d^d x, \tag{13}$$

and for the mean square displacement:

$$R^2(t) = \frac{\int x^2 t^{\eta - d\zeta/2} F(x^2/t^\zeta, \Delta t^{1/\nu_\parallel}) d^d x}{n_v(t)}. \tag{14}$$

TABLE II. Dynamic exponents of the one-dimensional model for some selected temperatures.

T	δ	η	ζ	Z
0.[18]	0.160(3)	0.314(2)	1.260(1)	1.54(5)
0.5	0.164(5)	0.308(3)	1.263(2)	1.590(7)
0.9	0.162(4)	0.313(3)	1.262(4)	1.575(6)
1.3	0.159(2)	0.311(2)	1.258(3)	1.56(2)
1.33	0.158(3)	0.314(2)	1.260(2)	1.584(8)
DP[25]	0.159464(6)	0.313686(8)	1.26523	1.580 745(10)

TABLE III. Spreading exponents and the ultimate-survival-probability exponent for three different initial conditions. ρ_{nat} stands for the initial concentration of A monomers obtained from the evolution rules of the model.

$\rho_{A,\text{ini.}}$	δ^*	η^*	ζ^*	β^*	$2(1+\beta/\beta^*)\delta^*+2\eta^*-\zeta^*$
$\rho_{\text{nat}}. = 0.108$	0.162(4)	0.313(3)	1.262(4)	0.273(6)	0.01(2)
0.4	0.101(2)	0.378(3)	1.268(2)	0.171(2)	0.01(3)
0.8	0.035(4)	0.472(5)	1.353(2)	0.059(3)	−0.01(5)

The exponents δ, η, and ζ in the last three equations are the dynamic critical exponents that we want to evaluate. At the critical point ($\Delta = 0$) these equations are reduced to

$$P_s(t) \approx t^{-\delta}, \tag{15}$$

$$n_v(t) \approx t^{\eta}, \tag{16}$$

$$R^2(t) \approx t^{\zeta}, \tag{17}$$

and we can find the exponents δ, η, and ζ from the straight-line behavior of the log-log plots of the quantities $P_s(t)$, $n_v(t)$, and $R^2(t)$ versus t, respectively. A key issue here is the choice of initial condition. Only one empty site at the center of the lattice is a mandatory requirement, but the other sites can be occupied by monomers of type A and B in several ways. For each value of temperature the configuration of the lattice is a composition of different concentrations of monomers A and B. The results we show below were obtained from an initial condition generated by the dynamic rules of the model, producing a natural configuration. We fixed T and started with an empty lattice, waiting for the complete coverage of the lattice. Then, the central site is made empty, and we restart the simulation to measure $P_s(t)$, $n_v(t)$, and $R^2(t)$. Later in this section we return to the discussion concerning the initial condition. In Fig. 5 we show the log-log plots of the quantities of interest for $T = 0.5$. The three curves shown are associated, from bottom to top, with the values $y_A = 0.6435$, $y_A = 0.6436$, and $y_A = 0.6437$. The central curve in each plot indicates the critical point and its slope gives the critical exponent. Then, we find that $\delta = 0.164(5)$, $\eta = 0.308(3)$, and $\zeta = 1.263(2)$. In Fig. 6 we show the results for the temperature $T = 0.9$. In this case the curves are associated with the values $y_A = 0.69$, $y_A = 0.692\,05$, and $y_A = 0.693$. From the slope of the central curves in each plot we have $\delta = 0.162(4)$, $\eta = 0.313(3)$, and $\zeta = 1.262(4)$.

In Table II we present the results for other values of temperature and for the dynamic exponent z. We also show in the table the best values of these dynamical exponents found for the DP universality class in one dimension. Once again, we also note that the dynamical exponents found in this work do not depend on temperature despite the initial configuration being dependent on it. The set of dynamical critical exponents of the present model are in close agreement with those of the DP universality class in one dimension.

Grassberger and de la Torre also showed that the spreading exponents should obey the hyperscaling relation

$$4\delta + 2\eta = d\zeta, \tag{18}$$

where d is the system dimensionality. From Table II it is clear that the exponents we have obtained follow the relation given by equation (18). We have also considered an arbitrary initial configuration that is different from the natural configuration of the system. Actually, the hyperscaling relation is obeyed only for the natural configuration. Consider, for instance, the case where we start the simulation with the lattice filled exclusively with monomers of type B except by its central site, which is left empty. For $T = 0.9$ the critical value of y_A remains the same (i.e., $y_A = 0.692\,05$); however, the exponents assume the following new values: $\delta = 0.182(6)$, $\eta = 0.286(4)$, and $\zeta = 1.250(4)$. These figures do not belong to the DP universality class and do not satisfy the hyperscaling relation (18). The same occurs starting with a lattice randomly filled with monomers of type A and B. Again, for $T = 0.9$, the critical point is not shifted, but the new exponents are $\delta = 0.076(3)$, $\eta = 0.402(4)$, and $\zeta = 1.248(6)$. The spreading exponents are clearly sensitive to the initial condition, changing with the concentration of monomers A and B. To deal with this surprising behavior, a generalized scaling theory was devised to allow the dynamic exponents to depend on the initial configuration [19]. This approach led to the generalized scaling relation

$$2\left(1+\frac{\beta}{\beta^*}\right)\delta^* + 2\eta^* = d\zeta^*, \tag{19}$$

where β is the usual DP exponent associated to the order parameter and the starred exponents are functions of the initial condition. The modified hyperscaling relation expression given by Eq. (19) was successfully applied to the dimer reaction model and to the threshold transfer process [19]. In order to illustrate this behavior in our model, we have determined the ultimate survival probability exponent β^* for three different initial conditions, including the natural one. The initial condition is characterized in terms of the concentration $\rho_{A,\text{ini}}$ of A monomers. In Table III we show the four exponents, and a test of the generalized hyperscaling relation for each initial condition and $T = 0.9$. Within the uncertainties, the generalized hyperscaling relation is verified. When $\rho_{A,\text{ini}} = \rho_{\text{nat}}$ we see that $\beta^* \simeq \beta$, and Eq. (19) is reduced to Eq. (18). For $\rho_{A,\text{ini}} \neq \rho_{\text{nat}}$ we have $\beta^* \neq \beta$, and the exponents must be related by the generalized Eq. (19).

VI. CONCLUSIONS

In this work we have studied a one-dimensional model of competitive reactions between two types of monomers (A and B) that exhibits a continuous phase transition from active to absorbing states. We have taken into account in our model the temperature of the catalyst as well as lateral interactions between pairs of nearest-neighbors monomers

adsorbed on the surface. For each value of temperature, the absorbing state is characterized by different concentrations of monomers A and B. We have calculated some ratios between moments of the order parameter of the system, which is the fraction of empty sites of the lattice. We have shown that the moment ratios do not depend on the temperature and are in close agreement with those calculated for the contact process. We have also determined the dynamic exponent z, which is related to the lifetime of the active states, and we have seen that it is also insensitive to changes in temperature, and its values are in accordance with the DP universality class. The spreading exponents δ, η, and ζ are clearly sensitive to the initial conditions. If the simulation is carried out from a system-generated initial configuration, which is a natural configuration of the model, the exponents assume the DP values and follow the usual hyperscaling relation. However, when we start the simulations with a nonnatural configuration as, for instance, $\rho_{A,\mathrm{ini}} \neq \rho_{\mathrm{nat}}$, we find new dynamical exponents that do not belong to the DP universality class. In this case, we have seen they satisfy the generalized hyperscaling relation, which is valid for arbitrary initial conditions.

ACKNOWLEDGMENTS

The authors would like to acknowledge the Brazilian agencies CAPES (PROBRAL and PNPD programs) and CNPq for financial support. This work is also partially supported by INCT-FCX (FAPESP-CNPq).

[1] M. F. de Andrade and W. Figueiredo, Phys. Rev. E **81**, 021114 (2010).
[2] H. K. Janssen, Z. Phys. B **42**, 151 (1981).
[3] P. Grassberger, Z. Phys. B **47**, 365 (1982).
[4] K. A. Takeuchi, M. Kuroda, H. Chaté, and M. Sano, Phys. Rev. Lett. **99**, 234503 (2007); **103**, 089901 (2009).
[5] K. A. Takeuchi, M. Kuroda, H. Chaté, and M. Sano, Phys. Rev. E **80**, 051116 (2009).
[6] M. Henkel, H. Hinrichsen, and S. Lubeck, *Nonequilibrium Phase Transitions, Vol.1: Absorbing Phase Transitions* (Springer, Bristol, 2008).
[7] E. T. Harris, Ann. Probab. **2**, 969 (1974).
[8] R. M. Ziff, E. Gulari, and Y. Barshad, Phys. Rev. Lett. **56**, 2553 (1986).
[9] Y. Pomeau, Physica D **23**, 3 (1986).
[10] D. Chowdhury, L. Santen, and A. Schadschneider, Phys. Rep. **329**, 199 (2000).
[11] I. Jensen, H. C. Fogedby, and R. Dickman, Phys. Rev. A **41**, 3411 (1990).
[12] J. W. Evans and M. S. Miesch, Phys. Rev. Lett. **66**, 833 (1991).
[13] E. V. Albano, Surf. Sci. **306**, 240 (1994).
[14] V. S. Leite and W. Figueiredo, Phys. Rev. E **66**, 46102 (2002).
[15] D. A. Browne and P. Kleban, Phys. Rev. A **40**, 1615 (1989).
[16] P. Meakin and D. J. Scalapino, J. Chem. Phys. **87**, 731 (1987).
[17] E. C. da Costa and W. Figueiredo, J. Chem. Phys. **117**, 331 (2002).
[18] E. C. da Costa and W. Figueiredo, Braz. J. Phys. **33**, 487 (2003).
[19] J. F. F. Mendes, R. Dickman, M. Henkel, and M. C. Marques, J. Phys. A Math. Gen. **27**, 3019 (1994).
[20] K. Binder, Phys. Rev. Lett. **47**, 693 (1981).
[21] R. Dickman and J. K. L. da Silva, Phys. Rev. E **58**, 4266 (1998).
[22] V. S. Leite, G. L. Hoenicke, and W. Figueiredo, Phys. Rev. E **64**, 036104 (2001).
[23] M. M. de Oliveira and R. Dickman, Phys. Rev. E **74**, 011124 (2006).
[24] P. Grassberger and A. de La Torre, Ann. Phys. **122**, 373 (1979).